ARTICLE

Local-friction governs water mobility in hydrogels acting as Extracellular mimics

Monojit Das,[a#] Jayanta Mondal,[b#] Naglaa Atif Alhadi Rahma,[b] Gourab Ghosh,[cd] Nivedita Pan,[b] Lopamudra Roy,[e] Ria Ghosh,[bf] Susmita Mondal,[b] Muhammad Munir,[g] Anjan Kumar Das,[h] Niko Hildebrandt,[g] Ranjan Das,[d*] Ranjit Biswas, [b *], Samir Kumar Pal,[bg*]

Received 00th January 20xx,
Accepted 00th January 20xx

DOI: 10.1039/x0xx00000x

[a.] *Department of Zoology, Vidyasagar University; Rangamati, Midnapore-721102, India*
[b.] *Department of Chemical and Biological Sciences, S. N. Bose National Centre for Basic Sciences; Block JD, Sector 3, Salt Lake, Kolkata-700106, India*
[c.] *Department of Chemistry, Vivekananda Mahavidyalaya, Haripal, Hooghly - 712405, India*
[d.] *Department of Chemistry, West Bengal State University, Barasat, Kolkata, India*
[e.] *Department of Applied Optics and Photonics, University of Calcutta; JD-2, Sector-III, Salt Lake, Kolkata, West Bengal, 700 106, India*
[f.] *Department of Biochemistry, University of Calcutta, 35, Ballygunge Circular Road, Kolkata 700019, India*
[g.] *Department of Engineering Physics, McMaster University, Hamilton, Ontario, L8S 4L7, Canada*
[h.] *Department of Pathology, Nil Ratan Sircar Medical College and Hospital; Kolkata-700014, India*

 # Equal contributions

Spectroscopic Characterization of RK-1 Probe

A Shimadzu UV-2600 spectrophotometer was used to record all the absorption spectra. All the steady-state emission and excitation spectra were recorded using a Jobin Yvon Fluorolog fluorimeter.

Differential Scanning Calorimetry (DSC) Analysis

The complex frequency (ν) dependent relative permittivity, $\varepsilon^*(\nu)$, is expressed as follows, (Böttcher, C. J. F.; Belle, O. C. van; Bordewijk, P.; Rip, A. Theory of Electric Polarization, Volume 2. 1978, 561. 10.1007/978-3-642-56120-7.)

$$\varepsilon^*(\nu) = \varepsilon'(\nu) - \left[i\varepsilon''(\nu) + \frac{ik}{2\pi\epsilon_0\nu}\right] \quad (1)$$

Where ϵ_0 is the permittivity of free space, k is the conductivity of the medium, and ε', ε'' denote the real and imaginary components of the complex permittivity.

Our experimental approach integrated two distinct setups:

(i) A low-frequency impedance analyzer (E4991B) with an open-ended coaxial probe (Keysight 85070E) and a high-temperature probe enabled measurements from 10 MHz to 500 MHz. Calibration was conducted with air, a shorting block, and water as open, short, and load standards, respectively.

(ii) A PNA-L network analyzer (N5235B) equipped with an open-ended coaxial probe kit (N1501A) to measure frequencies from 500 MHz to 50 GHz. Calibration for this setup also used air, a shorting block, and water as open, short, and load standards.

DR measurements were conducted in a laboratory with precise humidity control, maintained at approximately 30% relative humidity, and a stable ambient temperature of 298 K. Temperature stability was closely monitored using a thermometer positioned at the measurement site. Each measurement used a Chitosan hydrogel sample with a thickness of approximately 1 cm and a diameter of approximately 2 cm. These samples were designed to fully fill the measurement region and ensure stable mechanical properties. reducing edge effects and air-gap–induced scattering. The chosen thickness is suitable for broadband dielectric measurements and does not cause significant boundary or scattering issues or artifacts. Our

dimensions fall well within these guidelines. Special care was taken to ensure no air bubbles formed at the interface between the gel and the probe during measurement.

The dielectric response of the Chitosan hydrogel was analyzed by fitting the complex permittivity, $\varepsilon^*(\nu)$, to a sum of Havriliak-Negami (HN) relaxation functions[1]. The expression for the complex permittivity is:

$$\varepsilon^*(\omega) = \varepsilon_\infty + \sum_{j=1}^{n} \frac{\Delta\varepsilon_j}{\left[1 + \left(i2\pi\nu\tau_j\right)^{1-\alpha_j}\right]^{\beta_j}} - \frac{ik}{2\pi\epsilon_0\nu} \qquad (2)$$

where $0 \le \alpha < 1$ and $0 < \beta \le 1$. $\Delta\varepsilon_j$ denotes the amplitudes of the dispersion of j-th relaxation with time τ_j. Note that $\alpha_j = 0$ and $\beta_j = 1$ represents the relaxation via the Debye model, whereas $\alpha_j = 0$ with $\beta_j < 1$ describes the Cole-Davidson (CD), and $\alpha_j < 1 \beta_j = 1$ The Cole-Cole processes. Data collected from the dielectric measurements were simultaneously fitted using a multi-Debye relaxation model.

Fitting quality was estimated by checking the "goodness-of-fit" parameter (χ^2) determined using the following relation (Bevington; R., P. Data Reduction and Error Analysis for the Physical Sciences. *drea*1969.),

$$\chi^2 = \frac{1}{2m - l}\sum_{i=1}^{m}\left[\left(\frac{\delta\varepsilon_i^{'}}{\sigma\left(\varepsilon_i^{'}\right)}\right)^2 + \left(\frac{\delta\varepsilon_i^{''}}{\sigma\left(\varepsilon_i^{''}\right)}\right)^2\right] \qquad (3)$$

Where$m$is the number of data points $(\nu,\varepsilon^{'},\varepsilon^{''})$, l is the number of adjustable parameters, $\delta_{\varepsilon i}$ represents the residual for each data point, and $\sigma(\varepsilon_i)$ denotes the standard deviation. Lower values $\chi^2$of indicate a closer match between the fitted model and the experimental data, validating the applicability of the multi-Debye model to describe the relaxation behavior of the Chitosan hydrogel.

Femtosecond Resolved Fluorescence Measurements Using Streak Camera and Data Analysis:

Femtosecond-resolved fluorescence decay experiments were performed in a custom-made streak camera-based setup. A 3.5 ps FWHM, LASER source (Mai Tai HP 1040S from Spectra Physics, Mode-Locked Ti: sapphire Laser, 2.5 W, repetition rate 80 MHz) was used as a source for femtosecond pulses. The overall setup consists of a monochromator (SpectraPro HRS-300), a sample compartment, and a time profile is created using a streak sweep unit, along with a CCD camera from Optronics OPTOSCOPE SC-10, where the decay profile is recorded as an image, called a streak image. The second harmonic pulse of the original one (880 nm) was used as an excitation source when measuring the femtosecond time-resolved spectra.

The streak images consist of wavelength and time-resolved data recorded at a single frame. The x-axis of the image represents time resolution, ranging from 0 to 290 ps, whereas the y-axis spans 150 nm in wavelength. The decay profiles at narrow wavelength spans can be resolved by streaking out a window of specified width along the time axis (x-axis), and height along the wavelength axis (typically 1-5 nm). Similarly, the time-resolved emission spectra at a particular time span can be extracted by streaking a window of specified width along the wavelength axis (y-axis), and height along the time axis (typically 0-5ps).

a) Fitting of the decay profile:

The decay profiles constructed from streak images were exported and fitted using Micromath Scientist software. Typically a decay profile follows the equation below,

$$I(t) = I_0 e^{-\frac{1}{\tau}}, \qquad (4)$$

where, I(t) is the recorded intensity, I_0 is the initial intensity, and τ is the fluorescence lifetime. The above expression was modified for multiexponential fluorescence decays. To fit the multiple decay components, we follow iterative deconvolution, which employs a deconvolution technique based on a nonlinear least-squares process. Detailed fitting procedures are explained in "Principles of Fluorescence Spectroscopy" by Lakowicz [2]

Fitting of the time-resolved emission spectrum:

The "raw" time-dependent emission spectra are first converted from a wavelength representation to a frequency representation, where it is worth mentioning that the conversion between wavelength and frequency representations is done by reweighting intensity values by the factor $\frac{\Delta\lambda}{\Delta\nu} = \nu^2$. The data points determining the time-dependent emission spectra rarely follow a symmetric Gaussian distribution; rather, it follows skewed distribution and are fit to a log-normal line shape function [3].

Pico-Second-Resolved Fluorescence Measurements Using TCSPC and Data Analysis:

Picosecond time-resolved spectroscopic studies were conducted using a commercial time-correlated single-photon counting (TCSPC) setup from Edinburgh Instruments. A picosecond pulsed LASER of 510 nm wavelength was used as the excitation source in this study. The instrument response function was 80-100 ps. The experimental setup and methodology were discussed in detail in our earlier publications [4].

a) Construction of Picosecond Time-Resolved Emission Spectrum:

The primary raw data consist of emission decays recorded at a series of wavelengths (in our case, at 5 nm intervals) spanning the steady-state emission spectrum from blue to red over a definite interval (here, 5 min). As expected, the contour collected in this method would contain the time-resolved emission spectrum. The result of our interest was extracted from the contour spectrum, with data points from 0 to 7 ns and an interval of 0.05 ns. As mentioned in the previous section, the obtained time-dependent emission spectrum (TRES) was first converted from the wavelength (nm) domain to the frequency domain and fitted using a lognormal distribution.

b) The solvation correlation function (c(t)):

The solvation relaxation is accompanied by the time-dependent shift in the probe's emission peak with time. C(t) represents the plot between the emission maximum (i.e., the maximum of the value obtained by fitting the emission spectrum by the lognormal function [3] and the corresponding time.

$$C(t) = \frac{\nu(t) - \nu(\infty)}{\nu(0) - \nu(\infty)} \qquad (5)$$

Time-Resolved Fluorescence Anisotropy:

For the anisotropy measurements r(t), the parallel and perpendicular emissions were adjusted and aligned to the excitation, respectively, with respect to the polarizer at the emission side. r (t), calculated, was done following the equation below:

$$r(t) = \frac{I_{\parallel}(t) - G.I_{\perp}(t)}{I_{\parallel} + 2.G.I_{\perp}(t)} \qquad (6)$$

where $I_{\parallel}(t)$ and $I_{\perp}(t)$ are fluorescence decays of the dye at perpendicular and parallel polarized angles, respectively, corresponding to vertically polarized excitation light. G is an instrument grating factor, a wavelength-dependent instrument correction factor to compensate for the polarization bias of the detection system. The magnitude was obtained by a long tail matching technique [5].

The decay of anisotropy (r(t)) has been modelled by a bi-exponential decay function

$$r(t) = r_0(\beta_1 \exp\left(-\frac{t}{\varphi_1}\right) + \beta_2 \exp\left(-\frac{t}{\varphi_2}\right)) + k \qquad (7)$$

where r_0 is the initial anisotropy, φ1 and φ2 are the faster and slower rotational relaxation times, respectively, with β1 and β2 being their corresponding amplitudes, and k is a constant.

When the bi-exponential decay function is recast according to the 'Wobbling-in-a-cone' model

$$r(t) = r_0((1 - S^2)\exp\left(-\frac{t}{\varphi_1}\right) + S^2\exp\left(-\frac{t}{\varphi_2}\right)) \quad (8)$$

the order parameter 'S' recovered from the anisotropy decay data ($where\ S^2 = \beta_2$) can provide information on local environment of the probe particularly in micelles _ENREF_5[6]. In the wobbling-in-cone model, the semi-cone angle θ_c is obtained from the relation [6].

$$\theta_c = \cos^{-1}[\frac{1}{2}\left\{(1 + 8|S|)^{\frac{1}{2}} - 1\right\}] \quad (9)$$

Supplementary Figures

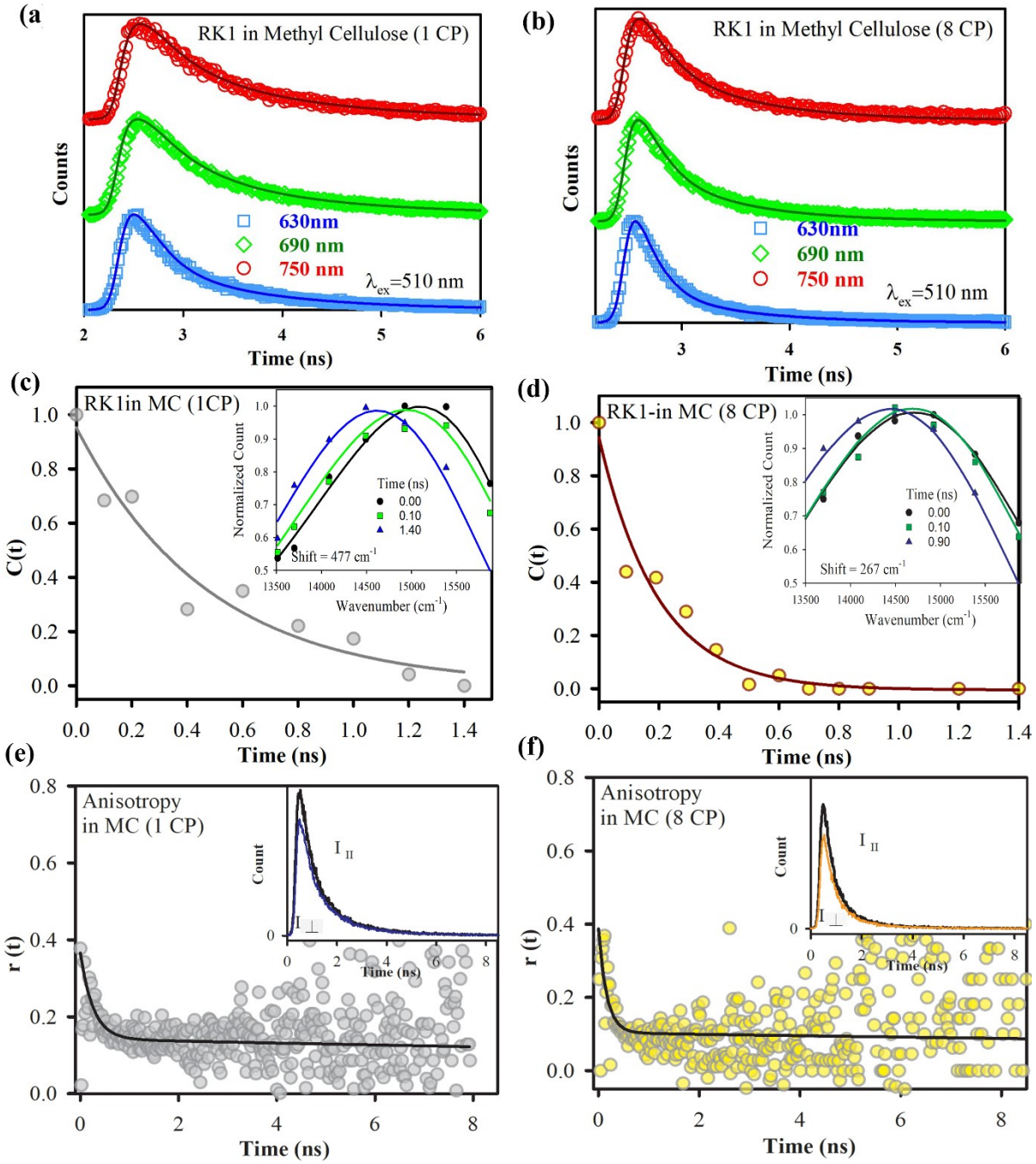

156

157 **Figure S1:** (a, b) represents the picosecond-resolved fluorescence decay transients of RK1 in methylcellulose at
158 the two different viscosities (1 CP and 8 CP), recorded at blue (630 nm), green (690 nm), and red (750 nm). (c,
159 d) The time evolution of the c(t) of RK1 up to several nanoseconds in methylcellulose 1 CP, and 8 CP
160 viscosities, TRES (inset) at three delay times, from the initial time 0, and at longer times 3obtained from
161 TCSPC. (e, f) The corresponding time-resolved nanosecond anisotropy r(t), the parallel and perpendicular
162 decay profile, is given in the inset of each part.

163

164

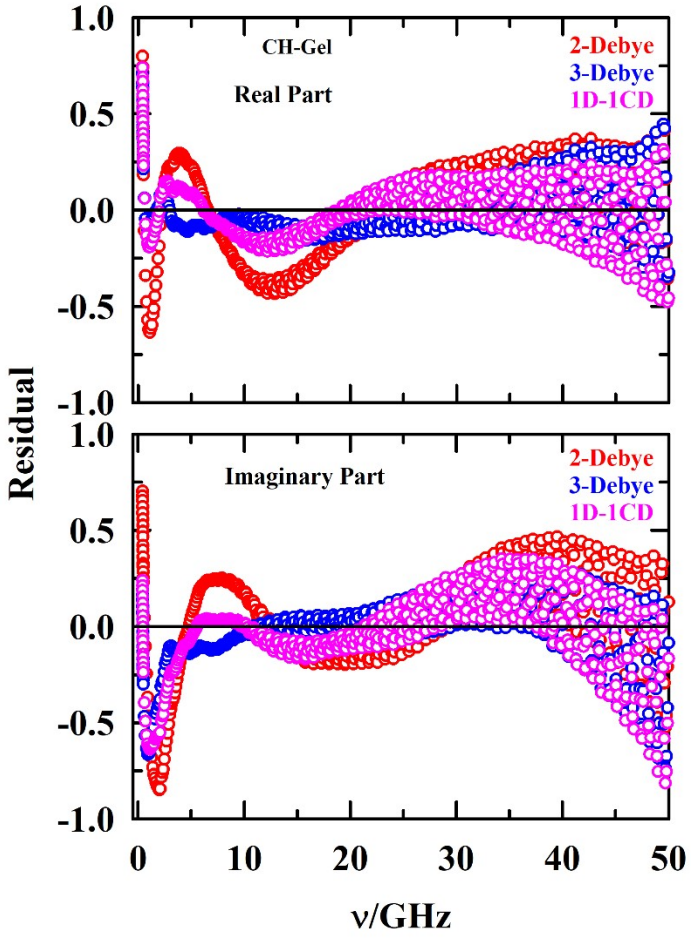

165

166 **Figure S2.** Residual comparison among 1-Debye, 2-Debye and 1D-1CD fits to the measured DR spectra for
167 chitosan hydrogel at 298 K. The representations are color-coded.

168

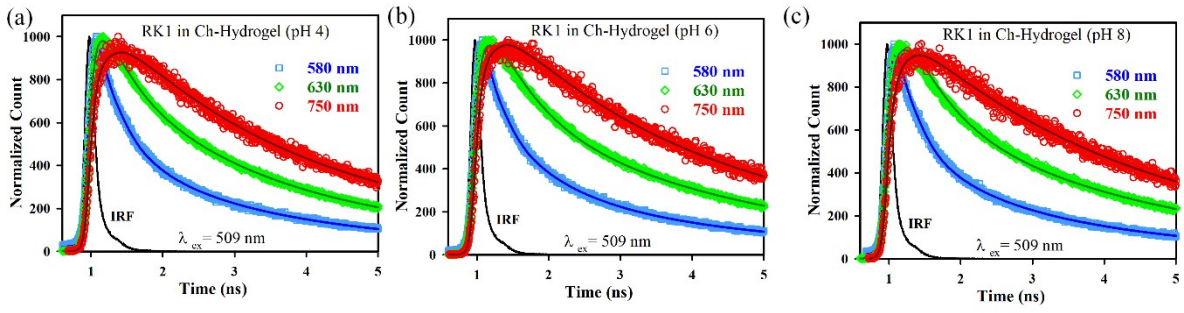

169

170 **Figure S3:** Represents the picosecond resolved fluorescence decay transients of RK1 in ch-hydrogel at the three
171 different pH levels (4, 6, 8), recorded at blue (580 nm), green (630 nm), and red (750 nm).

172

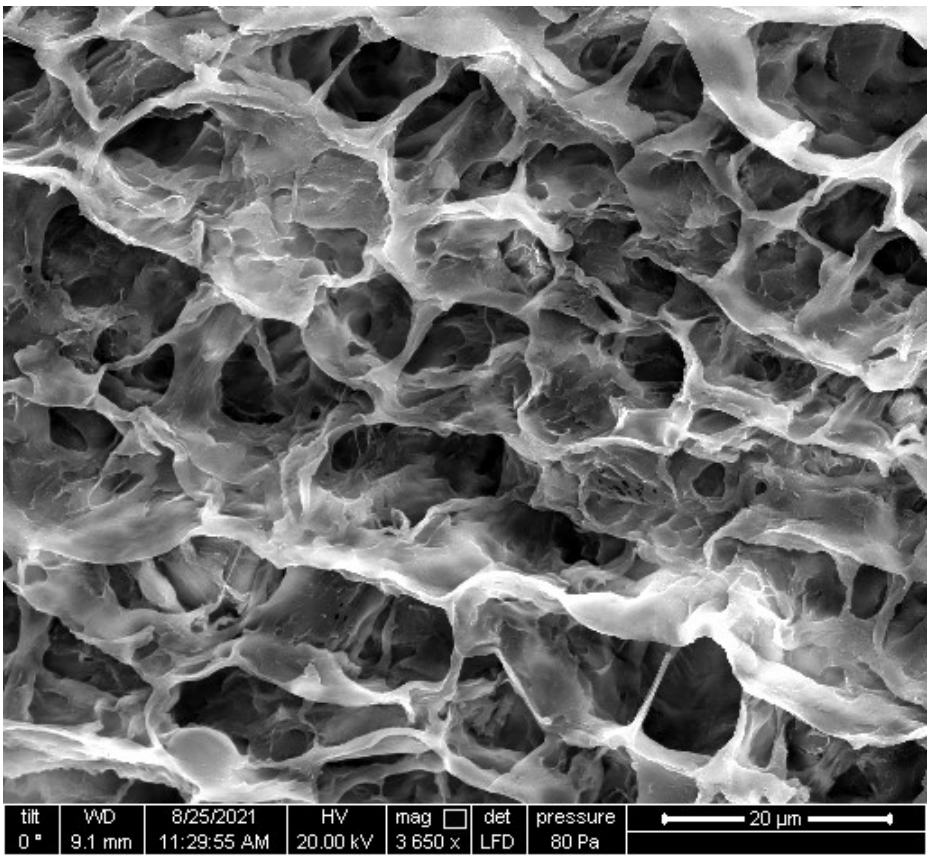

Figure S4: SEM image of the cross-sectional morphology of the chitosan hydrogel after lyophilization

Table S1: Decay Parameters obtained by fitting up to several nanoseconds: τ_1, represents rise, whereas τ_2, and τ_3 represents decay, their contribution is depicted in the parenthesis

System	Wavelength (nm)	τ_1 (ps) (%) rise	τ_2 (ps) (%) decay	τ_{avg} (ps) decay
RK1 in Methyl Cellulose-Hydrogel (1 CP)	630	250 (71%)	1160 (29%)	510
	690	400 (66 %)	1330 (33%)	710
	750	407 (65 %)	1400 (34%)	780
RK1 in Methyl Cellulose-Hydrogel (8 CP)	630	130 (84%)	770 (36%)	230
	690	160 (72 %)	770 (27%)	329
	750	180 (62 %)	790 (38%)	408

Table S2. Decay characteristics of the solvent response function C(t) constructed from TCSPC measurements, of RK1 in Methyl Cellulose at two different concentrations:

System	$\Delta\nu$ (cm^{-1})	τ_1 (ps) (a_1%)
1 CP	477 cm^{-1}	470
8 CP	267 cm^{-1}	190

Table S3: Time-resolved anisotropy r(t) parameters of methyl cellulose at different viscosities:

System	τ_1 (ps)	τ_2 (ns)
1 CP	260 (61 %)	50.0 (39 %)

8 CP	160 (73 %)	50.0 (27 %)

191

192 **Table S4. Decay Parameters of RK1 in chitosan hydrogel obtained by fitting up to several**
193 **nanoseconds: τ_1, represents the rise, whereas τ_2, and τ_3 represent decay; their contribution is**
194 **depicted in the parenthesis**

System	**Wavelength (nm)**	**τ_1 (ps) (%) (rise)**	**τ_2 (ps) (%) (decay)**	**τ_3 (ps) (%) (decay)**	**τ_4 (ps) (%) (decay)**
pH 4	580		150 (57 %)	750 (23 %)	3000 (20 %)
	630		450 (30 %)	1400 (34 %)	3800 (35 %)
	750	450 (14 %)		650 (20 %)	3800 (66 %)
pH 6	580		150 (58%)	850 (23 %)	3500 (19 %)
	630			600 (45 %)	3500 (55 %)
	750	400 (15 %)		1300 (18 %)	4800 (67 %)
pH 8	580		150 (54 %)	930 (21 %)	3500 (24 %)
	630			700 (33 %)	3500 (66 %)

	750	800 (6 %)		2300 (53 %)	5000 (4 %)

References:

1. F. Kremer and A. Schönhals, *Broadband dielectric spectroscopy*, Springer Science & Business Media, 2002.
2. J. R. Lakowicz, *Principles of fluorescence spectroscopy*, Springer, 2006.
3. M. Horng, J. Gardecki, A. Papazyan and M. Maroncelli, *The Journal of Physical Chemistry*, 1995, **99**, 17311-17337.

4. M. Das, S. Mondal, R. Ghosh, S. Darbar, L. Roy, A. K. Das, D. Pal, S. S. Bhattacharya, A. K. Mallick and J. K. Kundu, *Journal of Biomedical Materials Research Part A*, 2024.
5. G. F. Schröder, U. Alexiev and H. Grubmüller, *Biophysical journal*, 2005, **89**, 3757-3770.
6. K. Kinosita, A. Ikegami and S. Kawato, *Biophysical journal*, 1982, **37**, 461-464.

240

241

242

243

244

245

246

247

248

249

250

251